

# The depth of molecular recognition: voltage-sensitive blockage of synthetic multifunctional pores with refined architecture†

Yoann Baudry,<sup>a</sup> Dario Pasini,<sup>ab</sup> Masamichi Nishihara,<sup>‡a</sup> Naomi Sakai<sup>a</sup> and Stefan Matile<sup>\*a</sup>

Received (in Cambridge, UK) 8th July 2005, Accepted 9th August 2005

First published as an Advance Article on the web 5th September 2005

DOI: 10.1039/b509610c

Voltage-sensitive blockage by ADP, ATP and phytate (IP<sub>6</sub>) demonstrates that active-site contraction toward the middle of newly synthesized rigid-rod  $\beta$ -barrels provides a general strategy to rationally create and modulate the voltage sensitivity (and to increase the efficiency) of molecular recognition by synthetic multifunctional pores.

The key contribution of synthetic multifunctional pores<sup>1,2</sup> to the field of synthetic ion channels and pores<sup>3–18</sup> is the possibility to combine molecular translocation across lipid bilayer membranes with molecular recognition and transformation. The practical usefulness of synthetic multifunctional pores as substrate-independent transducers of chromophore-free molecular transformations into light has been demonstrated,<sup>15</sup> their ability to sense sugar in soft drinks illustrates their potential with regard to multicomponent sensing in complex matrices.<sup>16</sup> The design of synthetic multifunctional pores has, however, so far been limited to rigid-rod  $\beta$ -barrels with identical  $\beta$ -strands.<sup>1,2</sup> To overcome this limitation, we here describe design, synthesis and evaluation of synthetic multifunctional pore **1** with central and peripheral domains of different composition and dimension (Fig. 1). Four central RH dyads and two peripheral NN dyads per  $\beta$ -strand were positioned at the internal surface of rigid-rod {242}- $\beta$ -barrel **1**. This internal active-site contraction, compared to the classical pore **2** with RH dyads only, was envisioned for molecular recognition in the middle of pore **1** in the middle of lipid bilayer membranes. In the following, this “in-depth” guest inclusion is shown to provide access to, according to the Woodhull model,<sup>19,20</sup> the rational design of voltage-sensitive molecular recognition. Whereas several examples for the already challenging voltage-sensitive formation of synthetic ion channels and pores are available (e.g., push–pull rigid-rod  $\beta$ -barrels),<sup>4</sup> voltage-sensitive molecular recognition by synthetic ion channels and pores has, although similarly common in nature, so far not been realized “in depth”.<sup>4,13,14,17,18</sup>

The {242}-pore **1** was synthesized from commercial amino acids and biphenyls in overall 31 steps (Scheme 1, including routine<sup>21–23</sup> pentapeptide synthesis). The route to {242}-*p*-octiphenyl **3** with orthogonal acid protecting groups along the rigid-rod scaffold has been described previously.<sup>24,25</sup> Hydrogenolysis of the peripheral

benzyl esters of {242}-rod **3** liberated the four carboxylic acids for coupling with the N-termini of the side-chain protected LNLNL-pentapeptides. Subsequent acidic hydrolysis of the central *t*-butyl esters, coupling with side-chain protected LRLHL-peptides and side-chain deprotection gave the target rod **4** for self-assembly of pore **1** in lipid bilayer membranes.

The classical synthetic multifunctional pore **2** with uniform internal RH dyads has been characterized extensively in both spherical and planar bilayer membranes.<sup>21–23</sup> The active-site

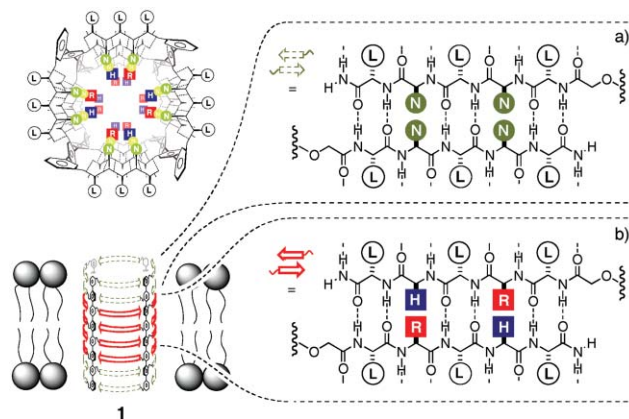
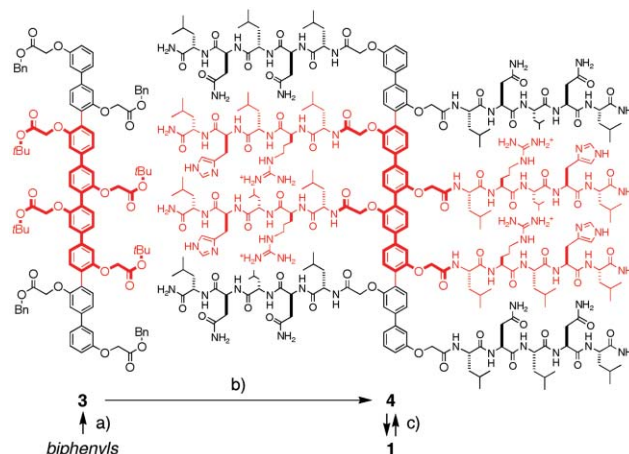


**Fig. 1** Notional rigid-rod  $\beta$ -barrel pore **1** with  $\beta$ -sheets as solid (backbone) and dotted lines (hydrogen bonds, *top*) or as arrows (N  $\rightarrow$  C, *bottom*); external amino-acid residues are dark on white, internal ones white on dark (single-letter abbreviations); pore **2**: analog to **1** with sequence b) only.



**Scheme 1** (a) See ref. 24; (b) sequential selective deprotection and peptide coupling, see ESI†; (c) self-assembly in lipid bilayers, see text.

<sup>a</sup>Department of Organic Chemistry, University of Geneva, Geneva, Switzerland. E-mail: stefan.matile@chiorg.unige.ch; Fax: +41 22 379 5123; Tel: +41 22 379 6523

<sup>b</sup>On leave from the Department of Organic Chemistry, University of Pavia, Pavia, Italy

† Electronic supplementary information (ESI) available: Experimental details. See <http://dx.doi.org/10.1039/b509610c>

‡ Current address: Kanagawa Academy of Science and Technology, Takatsu-ku, Kawasaki-shi, Japan.

contraction in refined pore **1** had overall little influence on the characteristics of pore **2**. According to the routine ANTS/DPX assay, pore activity decreased,<sup>§</sup> and the pH profile of both pores showed high activity at low pH with pH-gated opening at pH 5. In this assay, the fluorophore 8-aminonaphthalene-1,3,6-trisulfonate (ANTS) and the quencher *p*-xylylenebis(pyridinium) (DPX) are loaded into large unilamellar vesicles composed of egg yolk phosphatidylcholine (*i.e.*, EYPC-LUVs  $\Rightarrow$  ANTS/DPX). Efflux of either anionic ANTS or cationic DPX through the added pore is then observed as an increase in the emission intensity of ANTS (Fig. 2A a, dotted). With the same assay, molecular recognition by {242}-pore **1** could be observed as decreasing pore activity with increasing guest concentration (Fig. 2A a, dotted vs. solid). ADP, ATP and IP<sub>6</sub> (phytate) were selected as model blockers with increasing formal charge  $z_{\text{GUEST}}$ . Their inhibitory concentrations (IC<sub>50</sub>) or “apparent” dissociation constants ( $K_{\text{D}}$ ) revealed an exponential dependence of molecular recognition on formal guest charge (Fig. 2B). This trend was in excellent agreement with earlier insights on pore blockage by shape-persistent rigid-rod  $\alpha$ -helix mimics.<sup>26</sup> However, no such dependence was observed with regard to the formal charge of the supramolecular hosts. In the contrary,  $K_{\text{D}}$ 's obtained with refined pore **1** were consistently about half as large as those of classical pore **2** (Fig. 2B). This 2-fold increase in

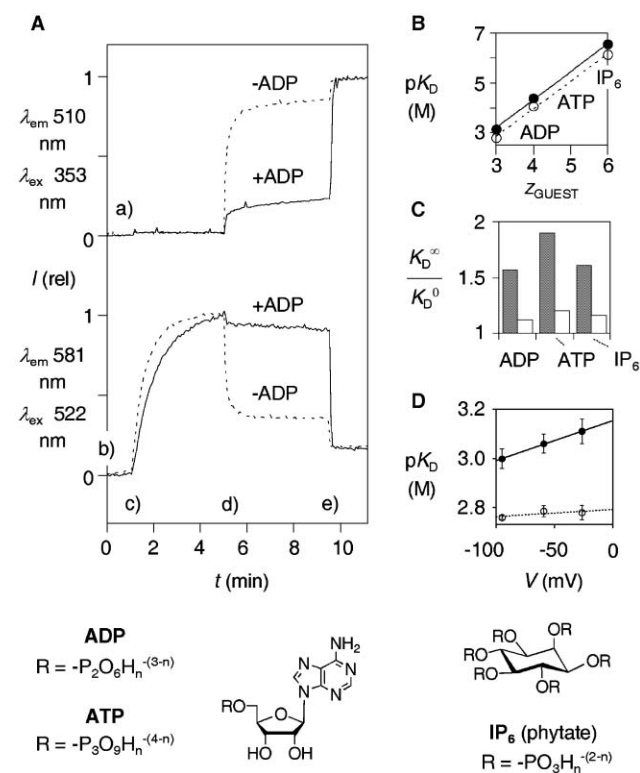


**Fig. 2** (A) Fractional change in emission  $I$  of (a) ANTS and (b) safranin O as a function of time during addition of valinomycin (c, 60 nM final), pore **1** (d, 250 nM tetramer) and Triton X-100 (e, excess) to EYPC-LUVs  $\Rightarrow$  ANTS/DPX (65  $\mu$ M EYPC, 10 mM MES, 100 mM NaCl, pH 4.5) in the presence (solid) or absence (dotted) of 4 mM ADP. (B) Apparent  $pK_{\text{D}}$ 's for blockage of pores **1** (●) and **2** (○) by ADP, ATP and IP<sub>6</sub> ( $pK_{\text{D}} = -\log K_{\text{D}}$ ). (C) Same with  $K_{\text{D}}^{\infty}$ 's for **1** (■) and **2** (□) in unpolarized compared to  $K_{\text{D}}^0$ 's in fully polarized vesicles. (D) Dependence of apparent  $pK_{\text{D}}$ 's for blockage of pore **1** (●) and **2** (○) as a function of vesicle polarization with fit to the Woodhull eqn (1).

molecular recognition upon active-site contraction validated our previous suspicions<sup>18</sup> that the depth of guest inclusion, that is *the location of the active site rather than the number of charges* determines molecular recognition by synthetic multifunctional pores.

Conductance experiments in planar EYPC bilayers revealed single conductance levels for {242}-pore **1** that were less inert and less homogenous than those of the classical pore **2** (Fig. 3A).<sup>21</sup> The corrected<sup>27,20</sup> small single pore diameter  $d = 7.0 \text{ \AA}$  calculated for refined pore **1** was indicative of counteranion immobilization by the internal arginine arrays as described previously for the similarly low-conducting classical pore **2**.<sup>21</sup>

The depth of molecular recognition is described in the Woodhull equation:<sup>19,20</sup>

$$K_{\text{D}} = K_{\text{D}}(0 \text{ mV}) \exp(l_{\text{W}} z F V / I R T) \quad (1)$$

This equation suggests that, with a given and constant length  $l$  of the pore, the exponential dependence of the dissociation constant  $K_{\text{D}}$  on the applied voltage  $V$  is determined by the charge  $z$  of the blocker as well as the Woodhull distance  $l_{\text{W}}$  from pore entrance to the active site within the pore. Here, an effective Woodhull distance  $l_{\text{W}}^{\text{eff}}$  is used to describe experimental values obtained with an assumed blocker charge  $z$ , whereas effective charges  $z_{\text{eff}}$  describe experimental values calculated from eqn (1) with an assumed Woodhull distance  $l_{\text{W}}$  (Table 1).

In multipore conductance experiments, ADP blocked the refined {242}-pore **1** in a voltage-dependent manner (Fig. 3B). Assuming a blocker charge  $z = -1.8$  for ADP at pH 4.5,<sup>28</sup> Woodhull analysis of this voltage dependence gave an effective Woodhull distance  $l_{\text{W}}^{\text{eff}} = 10.4 \text{ \AA}$  from pore entrance to active site (Table 1). Far beyond previous values obtained with classical pores ( $l_{\text{W}}^{\text{eff}} = 2.7 \text{ \AA}$ ),<sup>17,18</sup> this spectacular voltage sensitivity was in excellent agreement with the expected “in-depth” molecular recognition by refined {242}-pore **1** (theoretical  $l_{\text{W}} = 12.5 \text{ \AA}$ ).

Wondering about the exclusive focus on Woodhull analysis by conductance experiments in planar bilayers, we recently speculated that there is no obvious reason why the same shouldn't be possible and probably easier to reproduce in polarized spherical membranes.<sup>29</sup> To test this hypothesis, EYPC-LUVs  $\Rightarrow$  ANTS/DPX

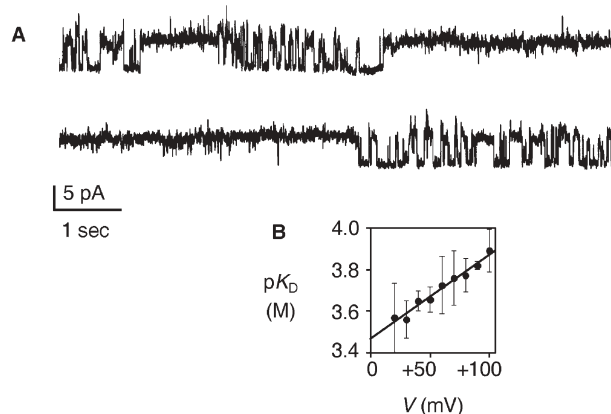


**Fig. 3** (A) Planar EYPC bilayer conductance in the presence of **1** (1  $\mu$ M *cis*) at  $V = +25 \text{ mV}$  (*trans* at ground) in 1.05 M KCl (5 mM MES, pH 4.65). (B) Woodhull plot for blockage of pore **1** with ADP ( $pK_{\text{D}} = -\log K_{\text{D}}$ ,  $K_{\text{D}} =$  dissociation constant, fit to eqn (1)).

**Table 1** Voltage dependence of pore blockage by ADP in spherical<sup>a</sup> and planar<sup>b</sup> bilayer membranes<sup>c</sup>

	pore <sup>d</sup>	$z\delta^{c,e}$	$z^{c,f}$	$l_W^{\text{eff}}/\text{\AA}^{c,g}$	$l_W/\text{\AA}^{c,h}$	$z_{\text{eff}}^{c,i}$
1 <sup>a</sup>	<b>2</b>	$-0.04 \pm 0.035$	-1.8	0.8	2.5	-0.6
2 <sup>a</sup>	<b>1</b>	$-0.22 \pm 0.008$	-1.8	4.2	12.5	-0.6
3 <sup>b</sup>	<b>1</b>	$-0.55 \pm 0.040$	-1.8	10.4	12.5	-1.5

<sup>a</sup> From polarized vesicles (Fig. 2). <sup>b</sup> From planar bilayer conductance (Fig. 3). <sup>c</sup> From Woodhull eqn (1),  $l_W^{\text{eff}}$  = experimentally determined Woodhull distance from pore entrance to active site obtained using an assumed blocker charge  $z$ ,  $F$  = Faraday constant,  $V$  = membrane potential,  $l$  = pore length (assuming 34 Å),  $R$  = gas constant,  $T$  = temperature. <sup>d</sup> Fig. 1. <sup>e</sup>  $\delta$  = electric distance =  $l_W^{\text{eff}}/l$ . <sup>f</sup>  $z$  = assumed charge of ADP at pH 4.5.<sup>28</sup> <sup>g</sup>  $l_W^{\text{eff}}$  = experimentally determined Woodhull distance obtained using  $z = -1.8$ . <sup>h</sup>  $l_W$  = Woodhull distance assumed from molecular models for detection of rate limiting binding to the first two available RH  $\beta$ -strands.<sup>17,18</sup> <sup>i</sup>  $z_{\text{eff}}$  = experimentally determined guest charge, from eqn (1) using the assumed Woodhull distances  $l_W$  in the preceding column.

were polarized as described previously by connecting a potassium gradient with the K<sup>+</sup>-carrier valinomycin.<sup>29,22</sup> For inside-negative polarization, potassium gradients were created by exchanging external K<sup>+</sup> with isoosmolar Na<sup>+</sup>/K<sup>+</sup> mixtures at ratios selected for the desired Nernst potentials. In double-channel fluorescence kinetics, changes in the membrane potential were monitored simultaneously with ANTS/DPX efflux (Fig. 2A, a) following the emission of the externally added safranin O (Fig. 2A, b). As with ANTS/DPX efflux, vesicle depolarization by pores **1** and **2** could be effectively inhibited with ADP (Fig. 2A b, solid vs. dotted), ATP and IP<sub>6</sub>. The found increase of the apparent  $K_D$  for refined pore **1** but not for classical pore **2** in polarized vesicles was consistent with blocker repulsion by the inside-negative membrane potential (Fig. 2C). Interference from stoichiometric binding<sup>30</sup> was likely to account for decreasing voltage sensitivity with excessive guest charge. Woodhull analysis of the voltage sensitivity of ADP revealed an  $l_W^{\text{eff}} = 4.2$  Å for the refined pore **1** that was clearly longer than the nearly negligible  $l_W^{\text{eff}} = 0.8$  Å for the classical pore **2** (Fig. 2D).

The  $l_W^{\text{eff}} = 4.2$  Å obtained in polarized vesicles was clearly shorter than the  $l_W^{\text{eff}} = 10.4$  Å obtained in planar bilayer conductance experiments (Table 1). The explanation of this difference with a reduced effective guest charge under these conditions was supported by the identical  $z_{\text{eff}} = -0.6$  obtained with the different expected  $l_W = 2.5$  Å and  $l_W = 12.5$  Å of pores **2** and **1**, respectively (Table 1). However, there was no clear-cut reason for this difference in  $z_{\text{eff}}$  beyond the general notion that different effective charges exist under different experimental conditions (e.g., ionic strength). Partial interference from the naturally voltage-independent ADP binding in the media was another meaningful explanation for the apparent underestimation of Woodhull distances in polarized vesicles. This explanation was consistent with the intrinsically poor detectability of this possibly competing process in planar bilayer conductance experiments. Whatever will turn out to be the reason for the different Woodhull distances in polarized vesicles and planar bilayer conductance experiments, we underscore that the essential lesson learned from the above experiments is that Woodhull analysis of the voltage dependence of molecular recognition by synthetic multifunctional pores as such is, at least in a more qualitative sense, possible in polarized vesicles.

In summary, the breakthroughs reported in this communication are (a) experimental evidence for synthetic access to refined pore architecture with distinct domains, (b) experimental evidence for voltage-sensitive “in-depth” blockage of synthetic ion channels and pores<sup>1–18</sup> and, from a methodological point of view, (c) experimental evidence that Woodhull analysis in polarized vesicles is possible.

We thank D. Ronan for assistance in synthesis, D. Jeannerat and A. Pinto for NMR measurements, P. Perrottet and the group of F. Gülaçar for MS measurements, two referees for helpful comments, and the Swiss NSF for financial support (including the National Research Program “Supramolecular Functional Materials” 4047-057496).

## Notes and references

§ Effective pore concentrations to observe 50% pore activity in the ANTS/DPX assay under the given conditions (pH 4.5, Fig. 2): EC<sub>50</sub> (**1**) = 140 nM, EC<sub>50</sub> (**2**) = 30 nM.<sup>23</sup>

- 1 N. Sakai and S. Matile, *Chem. Commun.*, 2003, 2514–2523.
- 2 N. Sakai, J. Mareda and S. Matile, *Acc. Chem. Res.*, 2005, **38**, 79–87.
- 3 R. S. Hector and M. S. Gin, *Supramol. Chem.*, 2005, **17**, 129–134.
- 4 S. Matile, A. Som and N. Sordé, *Tetrahedron*, 2004, **60**, 6405–6435.
- 5 K. D. D. Mitchell and T. M. Fyles, in *Encyclopedia of Supramolecular Chemistry*, ed. J. L. Atwood and J. W. Steed, Marcel Dekker, New York, 2004, 742–746.
- 6 G. W. Gokel and A. Mukhopadhyay, *Chem. Soc. Rev.*, 2001, **30**, 274–286.
- 7 W.-Y. Yang, J.-H. Ahn, Y.-S. Yoo, N.-K. Oh and M. Lee, *Nat. Mater.*, 2005, **4**, 399–402.
- 8 M. Yoshii, M. Yamamura, A. Satake and Y. Kobuke, *Org. Biomol. Chem.*, 2004, **2**, 2619–2623.
- 9 Y. J. Jeon, H. Kim, S. Jon, N. Selvapalam, D. H. Oh, I. Seo, C.-S. Park, S. R. Jung, D.-S. Koh and K. Kim, *J. Am. Chem. Soc.*, 2004, **126**, 15944–15945.
- 10 V. Sidorov, F. W. Kotch, J. L. Kuebler, Y.-F. Lam and J. T. Davis, *J. Am. Chem. Soc.*, 2003, **125**, 2840–2841.
- 11 Y. R. Vandenburg, B. D. Smith, E. Biron and N. Voyer, *Chem. Commun.*, 2002, 1694–1695.
- 12 J. M. Sanderson and S. Yazdani, *Chem. Commun.*, 2002, 1154–1155.
- 13 J. Sanchez-Quesada, M. P. Isler and M. R. Ghadiri, *J. Am. Chem. Soc.*, 2002, **124**, 10004–10005.
- 14 H. Ishida, Z. Qi, M. Sokabe, K. Donowaki and Y. Inoue, *J. Org. Chem.*, 2001, **66**, 2978–2989.
- 15 G. Das, P. Talukdar and S. Matile, *Science*, 2002, **298**, 1600–1602.
- 16 S. Litvinchuk, N. Sordé and S. Matile, *J. Am. Chem. Soc.*, 2005, **127**, 9316–9317.
- 17 B. Baumeister, N. Sakai and S. Matile, *Org. Lett.*, 2001, **3**, 4229–4232.
- 18 A. Som, N. Sakai and S. Matile, *Bioorg. Med. Chem.*, 2003, **11**, 1363–1369.
- 19 A. M. Woodhull, *J. Gen. Physiol.*, 1973, **61**, 687–708.
- 20 B. Hille, *Ionic Channels of Excitable Membranes*, 3rd edn, Sinauer, Sunderland, MA, 2001.
- 21 N. Sakai, N. Sordé, G. Das, P. Perrottet, D. Gerard and S. Matile, *Org. Biomol. Chem.*, 2003, **1**, 1226–1231.
- 22 N. Sordé and S. Matile, *J. Supramol. Chem.*, 2002, **2**, 191–199.
- 23 P. Talukdar, N. Sakai, N. Sordé, D. Gerard, V. M. F. Cardona and S. Matile, *Bioorg. Med. Chem.*, 2004, **12**, 1325–1336.
- 24 Y. Baudry, D. Ronan, D. Jeannerat and S. Matile, *Helv. Chim. Acta*, 2004, **87**, 2181–2189.
- 25 D. Jeannerat, D. Ronan, Y. Baudry, A. Pinto, J.-P. Saulnier and S. Matile, *Helv. Chim. Acta*, 2004, **87**, 2190–2207.
- 26 S. Litvinchuk and S. Matile, *Supramol. Chem.*, 2005, **17**, 135–139.
- 27 O. S. Smart, J. Breed, G. R. Smith and M. S. P. Sansom, *Biophys. J.*, 1997, **72**, 1109–1126.
- 28 E. M. Bianchi, S. A. A. Sajadi, B. Song and H. Sigel, *Chem. Eur. J.*, 2003, **9**, 881–892.
- 29 N. Sakai and S. Matile, *Chem. Biodiv.*, 2004, **1**, 28–43.
- 30 O. H. Straus and A. Goldstein, *J. Gen. Physiol.*, 1943, **26**, 559–585.